The *Salmonella* LysR family regulator, RipR, activates the SPI-13 encoded itaconate degradation cluster.

*Steven J. Hersch † and William Wiley Navarre **

Department of Molecular Genetics, University of Toronto, Toronto, Canada

†, Current address: Department of Ecosystem and Public Health, University of Calgary, Calgary, Canada

*, For correspondence: william.navarre@utoronto.ca

Abstract

Itaconate is a dicarboxylic acid that inhibits the isocitrate lyase enzyme of the bacterial glyoxylate shunt. Activated macrophages have been shown to produce itaconate, suggesting that these immune cells may employ this metabolite as a weapon against invading bacteria. Here we demonstrate that, *in vitro*, itaconate can exhibit bactericidal effects under acidic conditions similar to the pH of a macrophage phagosome. In parallel, successful pathogens including *Salmonella* have acquired a genetic operon encoding itaconate degradation proteins, which are induced heavily in macrophages. We characterize the regulation of this operon by the neighbouring gene, *ripR*, in specific response to itaconate. Moreover, we develop an itaconate biosensor based on the operon promoter that can detect itaconate in a semi-quantitative manner and, when combined with the *ripR* gene, is sufficient for itaconate-regulated expression in *E. coli*. Using this biosensor with fluorescence microscopy, we observe bacteria responding to itaconate in the phagosomes of macrophage and provide additional evidence that interferon-γ stimulates macrophage itaconate synthesis and that J774 mouse macrophages produce substantially more itaconate than the human THP-1 monocyte cell line. In summary, we examine the role of itaconate as an antibacterial metabolite in mouse and human macrophage, characterize the regulation of *Salmonella*'s defense against it, and develop it as a convenient itaconate biosensor and inducible promoter system.

Importance

In response to invading bacteria, immune cells can produce a molecule called itaconate, which can inhibit microbial metabolism. Here we show that itaconate can also directly kill

31 *Salmonella* when combined with moderate acidity, further supporting itaconate's role as an
32 antibacterial weapon. We also discover how *Salmonella* recognizes itaconate and activates a
33 defense to degrade it, and we harness this response to make a biosensor that detects the
34 presence of itaconate. This biosensor is versatile, working in *Salmonella enterica* or lab strains
35 of *Escherichia coli*, and can detect itaconate quantitatively in the environment and in immune
36 cells. By understanding how immune cells kill bacteria and how the microbes defend
37 themselves, we can better develop novel antibiotics to inhibit pathogens such as *Salmonella*.
38

39 **Introduction**

40 The mammalian immune system includes a multitude of weapons to defend against
41 invading microbes and successful pathogens have evolved a plethora of mechanisms to evade,
42 manipulate, or even benefit from these immune responses. One such pathogen, *Salmonella*
43 *enterica s*erovar Typhimurium (hereafter referred to as *Salmonella*), has acquired a number of
44 *Salmonella* pathogenicity islands (SPI) that support its survival inside of a host organism. For
45 instance, *Salmonella* employs SPI-1 to invade non-phagocytic cells, and SPI-2 allows the bacteria
46 to survive intracellularly – including in macrophage – which is important for *Salmonella*
47 virulence [1–4]. These traits allow *Salmonella* to invade the gut epithelium and induce intestinal
48 inflammation resulting in the characteristic gastroenteritis disease. Moreover, the induced
49 inflammation is not merely a threat that *Salmonella* must survive, but it has adapted to thrive in
50 the oxidative environment of the inflamed intestine and utilize inflammation-derived
51 metabolites to outcompete resident microbiota [5–7].

52 Itaconate (2-Methylenesuccinic acid, 2-Methylidenebutanedioic acid) is a metabolite
53 originally recognized in fungal species such as *Aspergillus terreus* and produced commercially
54 for use in polymer production [8–10]. As an unsaturated diacaboxylate that is somewhat similar in
55 structure to succinate, itaconate is a potent inhibitor of the glyoxylate shunt enzyme AceA
56 (isocitrate lyase) [11–13]. As such, itaconate inhibits bacterial growth on carbon sources such as
57 acetate and fatty acids, conditions that necessitate the glyoxylate shunt to generate the 4-
58 carbon skeletons that are critical for amino acid biosynthesis and central metabolism.
59 Interestingly, it has been demonstrated that activated macrophage employ the IRG1 protein to
60 produce itaconate, with higher concentrations being produced by mouse macrophage than
61 human [13–15]. Moreover, IRG1 closely associated with vesicles containing *Legionella pneumophila*
62 and itaconate showed bactericidal activity against this pathogen *in vitro* [15]. Itaconate was also
63 found to inhibit *Salmonella* growth by reducing media pH and itaconate levels in *Salmonella*-
64 infected mice correlated with splenomegaly [16]. Cumulatively, these works suggest that
65 itaconate acts as a weaponized metabolite that the immune system employs to inhibit the
66 growth of, or kill, invading bacteria.
67 If itaconate is an immune-derived antibacterial metabolite then it follows logically that
68 successful pathogens must have methods to evade its effects. Indeed an operon has been
69 identified in *Yersinia* (*ripABC* for 'required for intracellular proliferation') that encodes three
70 enzymes catalyzing the ATP/succinyl-CoA-dependent degradation of itaconate into pyruvate
71 and acetyl-CoA [17]. The operon is not restricted to *Yersinia* and a variety of other bacteria
72 including *Pseudomonas* encode homologs or functional analogs of these enzymes. Several
73 lineages of *Salmonella enterica* harbor a cluster of genes (e.g. genes STM3120-STM3117 in S.

74 Typhimurium strain LT2) within SPI-13 that we refer to here as the 'itaconate response operon'
75 (IRO). Interestingly, the IRO genes of *Salmonella* have been shown to be induced heavily in
76 macrophage but not under any other condition tested, supporting a role in degrading
77 macrophage-produced itaconate [18–20]. High throughput screens have suggested that genes from
78 this operon are important for *Salmonella* survival in mice [21–23]. Furthermore, it has also been
79 shown that SPI-13 is present in many generalist *S. enterica* serovars but not in some human-
80 restricted serovars of *Salmonella* (e.g. serovars Typhi and Paratyphi A, which encode SPI-8)
81 possibly due to reduced itaconate synthesis by human macrophages [24].
82 In this work we show that itaconate is bactericidal at low but not neutral pH and
83 elucidate the regulation of the *Salmonella* IRO and its induction in mouse and human
84 macrophage. We show that the promoter of the IRO (P_{IRO}) is specifically induced by itaconate
85 and that the LysR family transcriptional regulator encoded by the upstream gene, STM3121
86 (which we propose to name *ripR*), is both necessary and sufficient for this induction.
87 Furthermore, using P_{IRO} with a GFP reporter, we develop a semi-quantitative itaconate
88 biosensor and employ it to show that the IRO is induced heavily in the J774 mouse macrophage
89 cell line but requires interferon-γ (IFN-γ) stimulation to show a detectable response in the THP-1
90 human monocyte cell line.
91

92 **Results**

93 ***The* Salmonella *IRO is induced specifically by itaconate in a* RipR-*dependent manner***

94 The *Salmonella* pathogenicity island-13 includes genes encoding RipC/Ccl (STM3120 in
95 strain LT2), RipB/Ich (STM3119) and RipA/Ict (STM3118), whose homologs have been

96 demonstrated to degrade itaconate into pyruvate and acetyl-CoA [17]. This operon, which we
97 refer to as the itaconate response operon (IRO), appears to also include the STM3117 gene
98 (encoding a predicted glyoxalase-domain containing protein) and is adjacent to the STM3121
99 (*ripR*) gene on the reverse DNA strand (Figure 2).

100 The IRO is strongly induced in cultured mouse macrophages but, according to
101 expression data from SalCom and other published work, is seemingly independent of known
102 virulence regulators (PhoP, RpoS, SsrA/B, OmpR, SlyA, etc.). We hypothesized that itaconate
103 may act as an inducer of IRO expression via the adjacent LysR-family regulator encoded by
104 STM3121. To assess this, we constructed a plasmid-borne fusion of the operon's promoter
105 (P_{IRO}) to superfolder GFP (sfGFP) as a reporter[25]. Indeed, we found that the P_{IRO} promoter was
106 induced highly in the presence of itaconate and this response was entirely dependent on the
107 presence of RipR as neither a *Salmonella ripR* deletion mutant nor the same reporter plasmid in
108 *E. coli* K12 (which does not encode *ripR*) showed induction (Figure 3A). In contrast, when the
109 *ripR* gene was included on the reporter plasmid, itaconate-induced P_{IRO} expression was restored
110 in both the Δ*ripR Salmonella* strain and in *E. coli*. These data not only demonstrate that P_{IRO} is
111 induced in response to itaconate, but also that the neighbouring gene, *ripR*, is both necessary
112 and sufficient for this induction.

113 To assess if the IRO promoter is induced specifically by itaconate, we examined
114 induction of the P_{IRO} reporter plasmid in media supplemented with a panel of similar
115 metabolites. While mesaconate, citramalate and methylsuccinate (in order of induction
116 strength) slightly induced expression, induction by itaconate was drastically more pronounced,
117 suggesting that it is the principal inducer (Figure 3B). Notably, similar results were obtained in

118 complex media (LB) and in MOPS minimal media with either glucose or glycerol as a carbon
119 source, suggesting that the induction only requires itaconate and not additional factors in the
120 media (Figure S2). Furthermore, induction by itaconate occurred in a dose dependent manner
121 indicating that the reporter can be used to semi-quantitatively assess itaconate concentrations
122 encountered by the bacteria (Figure S3).
123

124 ***Itaconate import is independent of the dicarboxylate transporter DctA***

125 Another important question was whether or not itaconate required the primary aerobic
126 dicarboxylate transporter, DctA, for import into the cell. We compared itaconate-mediated
127 induction of the P_{IRO}-sfGFP reporter in wild-type or Δ*dctA Salmonella*. Interestingly, we found
128 that the IRO promoter was still heavily induced in the *dctA* mutant in the presence of itaconate
129 (Figure S4). This demonstrates that the DctA dicarboxylate transporter is not required for
130 itaconate-mediated induction of P_{IRO}, suggesting that itaconate import is independent of *dctA*.
131

132 ***Itaconate is bactericidal at low pH***

133 Previous work has demonstrated that itaconate can inhibit the function of the
134 glyoxylate shunt enzyme, AceA, and act as a bacteriostatic agent when bacteria rely on carbon
135 sources such as acetate that require this pathway [11–13]. It has also been suggested that
136 itaconate can inhibit bacteria by influencing media pH and at least one publication has
137 demonstrated that it can have bactericidal activity [15,16]. To clarify this later phenotype we
138 hypothesized that the dicarboxylic acid chemistry of itaconate would allow it to act in a
139 bactericidal fashion at low pH by acting as a proton shuttle. In brief, the carboxyl groups of

140 itaconate (pK_a = 5.5 and 3.8) protonate and lose their charge at lower pH allowing them to
141 traverse the bacterial membrane and release the protons in the more neutral pH of the
142 cytoplasm, thereby exacerbating acid stress (Figure 1A).

143 To emulate the intracellular conditions that *Salmonella* may encounter in a *Salmonella*
144 containing vacuole (SCV) of a macrophage we added itaconate to LPM media and then acidified
145 to pH 4.4, 5.0, or 5.8 to cover a range from the most acidic to more regular estimates of SCV pH
146 [26–28]. Indeed we found that wild-type *Salmonella* showed a 1000-fold decrease in survival after
147 3h hours at pH 4.4 with itaconate (Figure 1B). This lethality was alleviated at higher pH and also
148 occurred using a similar dicarboxylic acid, succinate. Importantly, the bactericidal effect was
149 also dependent on the presence of itaconate or succinate, as pH 4.4 LPM did not kill *Salmonella*
150 in the absence of a dicarboxylic acid (Figure S1A). Interestingly, deletion of the entire IRO
151 (STM3120-STM3117) or *aceA* had no effect, but deletion of the general stress response sigma
152 factor, RpoS (σ^{32}, σ^{S}), exacerbated *Salmonella's* sensitivity at both pH 4.4 and 5.0 (Figures 1C
153 and S1B). Cumulatively, these data demonstrate that itaconate or other dicarboxylic acids can
154 act in a bactericidal fashion under acidic conditions by exacerbating acid stress.

155

156 ***The* Salmonella *IRO does not significantly contribute to short-term survival in a mouse***
157 ***macrophage cell line***

158 The inhibitory effect of itaconate on AceA, its bactericidal activity under acidic
159 conditions, and the synthesis of itaconate in macrophage combine to support the concept that
160 these immune cells may be employing itaconate as an antibacterial compound. As a successful
161 pathogen, *Salmonella* has adapted to survive in activated macrophage and multiple previous

162 works have examined how IRO genes may influence *Salmonella* survival and virulence [21–23]. In
163 our hands, we found no significant reduction in survival of Δ*IRO* or Δ*ripR* strains in the mouse
164 J774 macrophage cell line (Figure S5). When the macrophages were pre-stimulated with IFN-γ,
165 there was a slight reduction in survival relative to wild-type, but this was not significant when
166 compared to an *aceA* mutant that showed no survival defect. In contrast, the growth of a *phoP*
167 deletion control strain was inhibited by macrophages even without IFN-γ.
168

169 **Salmonella *encounter itaconate in the phagosomes of mouse and IFN-γ-stimulated human***
170 ***macrophage***

171 Multiple high throughput studies have demonstrated that the IRO genes are induced
172 heavily in mouse macrophage [18–20]. Additional studies have identified itaconate in both mouse
173 and human macrophage but the mouse cells appear to produce significantly more of the
174 metabolite [13,14]. Furthermore, it has been demonstrated that interferon-β (IFN-β) and IFN-γ can
175 stimulate itaconate production in mouse macrophage [15,29–31].

176 To examine itaconate levels encountered by intracellular bacteria inside macrophage,
177 we employed our P_{IRO}-sfGFP reporter plasmid as a biosensor. By including a constitutively
178 expressed mCherry gene on the same plasmid, we could microscopically observe individual
179 bacteria inside macrophage and obtain semi-quantitative data by generating a GFP/mCherry
180 fluorescence ratio as an indicator of P_{IRO} induction and accordingly itaconate levels. Using this
181 system, we observed strong induction of the P_{IRO} promoter for wild-type *Salmonella* in J774
182 mouse macrophage and this signal was absent in the Δ*ripR* control (Figure 4). Furthermore, the
183 response could also be observed in *E. coli* if RipR was encoded on the same plasmid,

184 demonstrating that bacteria that are poorly adapted to intracellular survival also encounter
185 itaconate in macrophage.

186 In contrast to the mouse cell line, unstimulated human THP-1 monocytes showed
187 negligible itaconate levels as very few of the bacterial reporters showed any green fluorescence
188 above background levels (Figure 4). The bacteria did express the constitutive mCherry and
189 could be observed in the macrophage, suggesting that the lack of green fluorescence was not
190 due to decreased bacterial survival or protein expression. Stimulation of THP-1 cells with IFN-γ
191 (M1 activation), however, led to a significant increase in the green fluorescence of the reporter
192 bacteria in a RipR-dependent fashion. In contrast, itaconate levels in THP-1 cells induced with
193 IL-4 and IL-13 (M2 activation) resembled unstimulated cells (Figure S6).

194

195 **Discussion**

196 In this work we demonstrate that itaconate becomes bactericidal at acidic pH,
197 suggesting an additional mechanism for itaconate to act as an antibacterial metabolite beyond
198 inhibition of AceA. Thus, elevated itaconate levels in macrophage may act to inhibit bacterial
199 metabolism while also exacerbating acid stress on microbes in the phagosome. Protonation of
200 itaconate under acidic conditions may also grant it increased access to the bacterial cytoplasm
201 where de-protonation would trap the charged form close to its AceA target. This organic acid
202 killing effect has been demonstrated previously, including in a recent work showing propionate
203 inhibition of *Salmonella* in mice [32,33]. Of note, we also find that bacterial killing occurs with
204 succinate, a metabolite similar to itaconate that similarly increases in concentration in activated
205 macrophage [34]. Our findings that these dicarboxylic acids can kill *Salmonella* at pH 4.4 but not

206 higher may contribute to why *Salmonella* manipulates the SCV to maintain a pH closer to 5.0 in
207 order to avoid this organic acid stress. Moreover, they imply that organic acids such as
208 itaconate and succinate may contribute to the antibacterial activity of acidified phagosomes.

209 The antibacterial potential of itaconate, its synthesis in activated macrophage, and the
210 localization of IRG1 to bacteria-containing vacuoles, support its potential role as a weapon
211 against intracellular bacteria. Here we examined survival of *Salmonella* IRO or *ripR* deletion
212 strains in the mouse macrophage J774 cell line but saw no significant decrease in survival,
213 similar to a recent study examining SPI-13 in RAW264.7I macrophage [24]. However, in that work,
214 Espinoza *et al.* discovered that SPI-13 does play a role in *Salmonella* internalization into mouse
215 – but not human – macrophage [24]. Combined with previous works showing reduced survival of
216 IRO mutants in mice, this operon may play a more significant survival role in the context of
217 infection in animals that produce copious amounts of itaconate [20–23].

218 We find *Salmonella* responds to itaconate *in vitro* and intracellularly by strongly inducing
219 an operon encoding itaconate degradation proteins. This response is largely specific to
220 itaconate and is entirely dependent on the neighbouring gene (*STM3121* in the prototypical
221 *Salmonella enterica* Sv. Typhimurium strain LT2), which we propose to rename *ripR* ('rip operon
222 regulator') to conform to earlier nomenclature. The *ripR* gene product is predicated to be a LysR
223 family transcriptional regulator, suggesting that itaconate induces IRO expression by interacting
224 directly with the substrate binding domain of RipR to activate it. Moreover, we find that RipR is
225 sufficient for itaconate induction of the P_{IRO} promoter in *E. coli*, demonstrating its potential as a
226 novel inducible expression system with over 50-fold higher transcription in the presence of the
227 inexpensive and readily available inducer. A limitation of this expression system would be a

228 requirement for growth on carbon sources independent of the glyoxylate shunt and also
229 growth at neutral or alkaline pH, as we demonstrate that itaconate is bactericidal under acidic
230 conditions. However, for many studies these conditions are met, adding P_{IRO} to the repertoire
231 of available inducible promoter systems.

232 Using our P_{IRO}-sfGFP itaconate biosensor, we showed a pronounced response in
233 unstimulated mouse macrophage whereas no induction was observed in the THP-1 human
234 macrophage cell line without stimulation, suggesting that these cells are not producing
235 itaconate to the same degree. Interferon has previously been demonstrated to stimulate
236 itaconate production in mouse macrophage and we found that our biosensor was induced in
237 human cells stimulated with IFN-γ [15,29–31]. Thus, while the human cell line was able to produce
238 itaconate, it required auxiliary induction to do so and still produced less than the uninduced
239 mouse macrophage. While it is possible that this reflects an artifact of the cell lines employed, it
240 aligns well with previous works that quantified itaconate in both mouse and human cells [13,14].
241 Furthermore, Espinoza *et al.* recently determined that SPI-13 is abundant in generalist
242 *Salmonella* serovars but not human-restricted ones (which instead encode SPI-8), suggesting
243 that low itaconate levels in humans render the IRO dispensible in these strains [24].

244 A recent study demonstrated that small molecules can inhibit the activity of the IRO
245 proteins and sensitize *Salmonella* to itaconate inhibition in minimal media [35]. Such drugs could
246 also sensitise other bacteria to itaconate including *Yersinia, Pseudomonas* and *Mycobacteria*
247 species, which also encode an IRO [17,35]. Moreover, if human-restricted pathogens lack an IRO
248 because human cells truly produce less itaconate, then they are potentially sensitive to it and
249 itaconate itself could potentially be used as an antimicrobial against them. Our biosensor could

250 prove invaluable in such studies for determining how much itaconate the bacteria are
251 encountering, and the self-sufficiency of the biosensor allows it to be employed in a variety of
252 species, providing added versatility.

253 In summary, here we present data that itaconate can act as a bactericidal metabolite at
254 acidic but physiologically relevant pH. We identify the regulatory mechanism of an itaconate
255 response operon in *Salmonella* and employ its promoter as a novel biosensor of relative
256 itaconate concentrations in macrophage phagosomes. Finally, we provide further evidence that
257 IFN-γ stimulates itaconate synthesis and moreover that human cells produce less of the
258 metabolite than their mouse equivalents.

259

260

261 **Materials and Methods**

262 ***Bacterial strains and plasmids***

263 All *Salmonella* strains used in experiments are derivatives of *Salmonella enterica subsp.*
264 *enterica* serovar Typhimurium (*S.* Typhimurium) strain 14028s. As described previously, lambda
265 red recombination and subsequent P22 phage transduction was used to generate all of the
266 gene knockout mutants in this background [36–38]. To allow for subsequent recombinations, the
267 antibiotic resistance cassette was removed from the chromosome using the pCP20 plasmid
268 encoding FLP recombinase [39]. The heat-unstable pCP20 plasmid was eliminated by passaging
269 overnight at 42°C and loss was confirmed by antibiotic treatment.

270 A reporter fusion of the IRO promoter to sfGFP (P_{IRO}-sfGFP) was generated using Gibson
271 cloning to insert the 333bp upstream of the STM3120 start codon (thereby including 25bp

272 upstream of the predicted -35 box and the 5' untranslated region) into the pXG10sf plasmid
273 (replacing the existing promoter)[40–42]. For the reporter construct including *ripR*, the same
274 region was extended to 1570bp upstream of the STM3120 start codon to include the entire
275 STM3121 ORF and a predicted transcriptional terminator following it. For fluorescence
276 microscopy, constitutively expressed (PLtet0-1 promoter) mCherry was inserted into a
277 transcriptionally independent region of the same plasmid. This variation of the plasmid was
278 renamed 'independent constitutive mCherry' or pICM.
279

280 ***Metabolite induction of P_{IRO} assay***

281 Induction of the *Salmonella* P_{IRO} promoter was assessed using a transcriptional fusion to
282 sfGFP in either the pXG10sf or pICM plasmids. Data from the two plasmids were combined as
283 the inducible region is identical and the plasmids only differ in the constitutively active mCherry
284 expressed independently on pICM. Overnight LB cultures were used to inoculate (1/200
285 dilution) either LB or MOPS minimal media containing 0.2% of the indicated carbon source.
286 Itaconate or other metabolites at neutral pH were supplemented to a concentration of 0.2%. Of
287 note, for salts and hydrates the final 0.2% concentration reflects the percent of the carbon
288 source itself; e.g. 0.2% succinate was made as 0.47% sodium succinate (dibasic) hexahydrate.
289 Growth was conducted in a TECAN Infinite M200 plate reader at 37°C with shaking and OD_{600}
290 and GFP fluorescence (475nm and 511nm excitation and emission wavelengths respectively)
291 were read every 15 minutes. For clarity, bar graphs show fluorescence at 16h post inoculation.
292 Chloramphenicol was included in all media at a concentration of 20µg/ml to maintain the
293 plasmids.

294

295 ***Acidified media survival***

296 LPM media was made as described previously [43,44]. Succinate or itaconate were added
297 to 0.4% and the pH was then adjusted to 4.4, 5.0 or 5.8 as indicated. LB overnight cultures were
298 resuspended in acidified media to an OD of 0.1 and incubated in a 37°C water bath. At time
299 points, samples were taken, serial diluted and plated for colony forming units (CFU).

300

301 ***Intra-macrophage survival***

302 The THP-1 human monocyte cell line and the J774 mouse macrophage cell line were
303 maintained in RPMI Medium 1640 (with L-glutamine) supplemented with 10% FBS and 1%
304 Glutamax and grown at 37°C and 5% CO_2. THP-1 cells were seeded in 96-well plates at 50,000
305 per well with 50nM PMA (phorbol 12-myristate 13-acetate) added to induce differentiation to
306 adherent macrophage. After 48h, media was replaced with no-PMA growth media overnight
307 with 100 U/ml human IFN-γ or IL-4 and IL-13 added if indicated. For J774 macrophage the cells
308 were seeded in 96-well plates at 50,000 per well overnight with 100 U/ml mouse IFN-γ added if
309 indicated. *Salmonella* in RPMI were added onto seeded cells at a multiplicity of infection (MOI)
310 of approximately 20:1 and centrifuged for 10 minutes at 1000 rpm to maximize cell contact.
311 After centrifuging the samples were incubated at 37°C and 5% CO_2 (time 0). After 30 minutes,
312 cells were washed three times with PBS followed by fresh media containing 100 µg/ml
313 gentamicin to kill extracellular *Salmonella*. At 2 hours the media was replaced with media
314 containing gentamicin at 10 µg/ml. At timepoints, intracellular bacteria were recovered using
315 PBS containing 1% Triton X-100 and vigorous pipetting. Samples were serially diluted and five

316 10µl spots were plated for CFU counting. Each sample included three separate wells as
317 technical replicates (a total of 15 x 10µl spots counted per biological replicate).
318
319 ***Fluorescence microscopy***
320 Fluorescence microscopy was conducted similarly to the macrophage survival assay with
321 some exceptions: Cells were seeded in 24-well plates containing glass coverslips at 125,000 per
322 well. Bacteria were infected at an MOI of approximately 100 to maximize the instances of
323 macrophage containing bacteria. At timepoints the media was removed and cells were washed
324 three times with PBS. They were then fixed for 10 minutes at room temperature in PBS + 4%
325 paraformaldehyde (PFA). Following three more PBS washes the cells were permeabilized for 10
326 minutes in PBS + 0.2% Triton X-100 + 1% BSA. Coverslips were washed again, mounted on slides
327 using 3µl mounting media containing DAPI and allowed to dry overnight in the dark. Slides
328 where viewed using a Zeiss Observer.z1 microscope using a 100x oil immersion objective and
329 the Zeiss Zen microscopy software. Images were taken with a Zeiss Axiocam 506 mono camera
330 mounted on the microscope. For all samples a 2s exposure was used for mCherry and 1s
331 exposure for sfGFP. ImageJ software was employed for quantification to calculate fluorescence
332 intensities in the red and green channels relative to a neighbouring background region for each
333 bacterium and a GFP/mCherry ratio was generated.
334
335 **Acknowledgements**
336 We would sincerely like to thank Dr. Scott Gray-Owen and members of his lab, in
337 particular Dr. Ryan Gaudet, for their generous donation of technical expertise, macrophage

338 cells lines, and use of their equipment. WWN was supported by an Operating Grant from the
339 Canada Institutes for Health Research (MOP-86683) and a Natural Sciences and Engineering
340 Research Council (NSERC) of Canada Grant (RGPIN 386286-10). SJH was supported by an NSERC
341 Vanier Canada Graduate Scholarship.

342

343 **Figure Legends**

344 **Figure 1: Itaconate is bactericidal at low pH. A)** At neutral pH, the charges on itaconate inhibit
345 diffusion across a lipid membrane (left). At acidic pH, itaconate protonates to itaconic acid,
346 which can traverse the membrane (right). In the cytoplasm, itaconic acid dissociates and
347 releases protons, trapping it in the cell and acidifying the cytoplasm. **B)** Survival (relative to 0h
348 time point) of wild-type (WT) or *rpoS* mutant *Salmonella* after 3h in LPM media supplemented
349 with 0.4% itaconate or succinate (Succ) and adjusted to pH 4.4, 5.0, or 5.8 as indicated. **C)** As in
350 A but showing survival of *Salmonella aceA* and itaconate response operon (IRO) mutants in LPM
351 + itaconate media at pH 4.4. All data are the average of at least three biological replicates and
352 error bars show one standard deviation. A one-way ANOVA with Sidak's multiple comparison
353 test was conducted comparing each sample to the same strain at pH 5.8 (B). WT in succinate
354 was compared to WT at pH 5.8 in itaconate. Mutants in panel C were not significantly different
355 than their parental strain (WT or Δ*rpoS*). ***, $p < 0.001$.

356

357 **Figure 2: Overview of the itaconate degradation operon (IRO) and the itaconate-responsive**
358 **regulator, *ripR*.** *Salmonella* gene loci based on the genome of *Salmonella* Typhimurium LT2 are
359 shown below. Identities of *ccl*, *ich*, and *ict* are shown above as previously reported [17]. STM3117

360 appears to be encoded in the same operon however its function remains unknown. In this work
361 we designate the names '*ripR*' for STM3121, 'itaconate response operon' (IRO) for STM3120-
362 STM3117, and 'P_{IRO}' for the IRO promoter.
363
364 **Figure 3: RipR is necessary and sufficient to induce P_{IRO} expression in response to itaconate.**
365 Expression of P_{IRO}-sfGFP in wild-type (WT) or *ripR* knockout (Δ*ripR*) *Salmonella*, or in *E. coli*.
366 Figures show GFP fluorescence normalized to optical density at 600nm (OD_{600}) after 16h of
367 growth in LB alone or supplemented with 0.2% itaconate (A) or similar metabolites (B). Data are
368 the average of at least three biological replicates and error bars show one standard deviation.
369 pP_{IRO}, plasmid-borne transcriptional fusion of P_{IRO} to sfGFP; pRipR-P_{IRO}, pP_{IRO} with the *ripR* gene
370 and its native promoter included on the plasmid. A Games-Howell ANOVA was conducted
371 comparing with and without itaconate for each strain (A), or comparing WT to Δ*ripR* (B) for
372 each added metabolite. *, $p < 0.05$; **, $p < 0.01$; ***, $p < 0.001$.
373
374 **Figure 4: P_{IRO} is activated in J774 macrophage and THP-1 macrophage stimulated with IFN-γ.**
375 Expression of P_{IRO}-sfGFP in intracellular wild-type (WT) or *ripR* knockout (Δ*ripR*) *Salmonella*
376 containing the pICM-P_{IRO} plasmid (constitutive mCherry expression). For expression in *E. coli,*
377 the *ripR* gene was also encoded on the reporter plasmid. '+ IFN-γ' samples were pre-treated
378 with human IFN-γ. **A)** Representative fluorescence microscopy images. **B)** Relative fluorescence
379 quantification of individual bacterial particles at 8h post-infection. Number of bacteria
380 quantified is indicated above and totalled from at least two biological replicates (≥ 3 for all WT
381 *Salmonella* samples). Boxes indicate first and third quartiles; central line, median; X, mean;

382 whiskers, 95th percentile; dots, all non-zero data points outside 95th percentile. The y-axis
383 changes scale at 1.5 to better show outliers. A Games-Howell ANOVA was conducted
384 comparing indicated samples. ***, $p < 0.001$.
385
386 **Supplemental Figure Legends**
387 **Figure S1: pH 4.4 without itaconate was not bactericidal. A)** Survival (relative to 0h time point)
388 of wild-type (WT) or *rpoS* mutant *Salmonella* after 3h in LPM media adjusted to pH 4.4, 5.0, or
389 5.8 as indicated. **B)** Survival of *Salmonella aceA* and itaconate response operon (IRO) mutants in
390 LPM + itaconate media at pH 5.0. All data are the average of at least three biological replicates
391 and error bars show one standard deviation.
392
393 **Figure S2: Itaconate induction of P_{IRO} occurs in minimal media.** Expression of P_{IRO}-sfGFP in
394 wild-type (WT) or *ripR* knockout (Δ*ripR*) *Salmonella* as in Figure 1 except grown in MOPS
395 minimal media with 0.2% Glucose (**A**; MGlu) or Glycerol (**B**; MGly) instead of LB. Data show GFP
396 fluorescence normalized to OD_{600} after 16h of growth and are the average of at least three
397 biological replicates. Error bars show one standard deviation. pP_{IRO}, plasmid-borne
398 transcriptional fusion of P_{IRO} to sfGFP. A Games-Howell ANOVA was conducted comparing WT
399 to Δ*ripR* for each added metabolite. *, $p < 0.05$; **, $p < 0.01$; ***, $p < 0.001$.
400
401 **Figure S3: P_{IRO} is induced by itaconate in a dose-dependent manner. A)** Example replicate
402 showing *Salmonella* optical density (dashed lines) and P_{IRO}-sfGFP fluorescence (solid lines) for a
403 range of itaconate concentrations across 16h of growth. All conditions were in MOPS minimal

404 media with 0.2% glucose as a carbon source and indicated concentration of itaconate (%,
405 g/100ml). **B)** Average P_{IRO}-sfGFP fluorescence (normalized to OD_{600}) at 8h or 16h across two
406 biological replicates. Error bars indicate one standard deviation. The x-axis changes scale at
407 0.0075% to show lower concentrations more clearly.
408
409 **Figure S4: DctA is not required for the response to itaconate.** Expression of P_{IRO}-sfGFP in wild-
410 type (WT) or *dctA* knockout (Δ*dctA*) *Salmonella*. Figure shows GFP fluorescence normalized to
411 optical density at 600nm (OD_{600}) after 16h of growth in MOPS minimal media with 0.2% glycerol
412 as the carbon source. Data are the average of at least two biological replicates and error bars
413 show one standard deviation. pP_{IRO}-sfGFP*,* plasmid-borne transcriptional fusion of P_{IRO} to sfGFP.
414
415 **Figure S5: Survival of *Salmonella* mutants in J774 macrophage with and without IFN-γ**
416 **stimulation** relative to wild-type. The fold change in CFU recovered (24h relative to 2h post-
417 infection) is shown and data from each replicate was normalized to the 24h/2h ratio obtained
418 for wild-type *Salmonella*. Columns show the average of three biological replicates and error
419 bars show one standard error of the mean. Since samples were normalized to wild-type in each
420 replicate, a one-way ANOVA with Sidak's multiple comparison test was conducted comparing
421 each strain to the Δ*aceA* strain (A) or to the Δ*rpoS* strain (B). Only the Δ*phoP* mutant was found
422 to have a $p < 0.05$. *, $p<0.05$; **, $p < 0.01$.
423
424 **Figure S6: P_{IRO} shows little-to-no activation in THP-1 macrophage stimulated with IL-4 and IL-**
425 **13.** As in Figure 4, expression of P_{IRO}-sfGFP in intracellular wild-type (WT) or *ripR* knockout

426 (Δ*ripR*) *Salmonella* containing the pICM-P_{IRO} plasmid (constitutive mCherry expression). THP-1
427 macrophage were pre-treated with no stimulant, human IFN-γ, or IL-4 and IL-13 and infected
428 with *Salmonella* for 8h. Data for WT *Salmonella* in THP-1 with no treatment or IFN-γ are shown
429 in Figure 4 and are shown again here for comparison. As in Figure 4, data shows relative
430 fluorescence quantification of individual bacterial particles. Number of bacteria quantified is
431 indicated above and totalled from at least three biological replicates. Boxes indicate first and
432 third quartiles; central line, median; X, mean; whiskers, 95th percentile; dots, all non-zero data
433 points outside 95th percentile. The y-axis changes scale at 1.5 to better show outliers.
434

435 **References**

436 1. Hansen-Wester, I. & Hensel, M. Salmonella pathogenicity islands encoding type III
437 secretion systems. *Microbes Infect.* **3**, 549–559 (2001).
438 2. Fields, P. I., Swanson, R. V, Haidaris, C. G. & Heffron, F. Mutants of Salmonella
439 typhimurium that cannot survive within the macrophage are avirulent. *Proc. Natl. Acad.*
440 *Sci. U. S. A.* **83**, 5189–5193 (1986).
441 3. Bäumler, A. J., Tsolis, R. M., Ficht, T. A. & Adams, L. G. Evolution of Host Adaptation in
442 Salmonella enterica. *Infect. Immun.* **66**, 4579–4587 (1998).
443 4. Bäumler, A. J., Kusters, J. G., Stojiljkovic, I. & Heffron, F. Salmonella typhimurium loci
444 involved in survival within macrophages. *Infect. Immun.* **62**, 1623–1630 (1994).
445 5. Thiennimitr, P. *et al.* Intestinal inflammation allows Salmonella to use ethanolamine to
446 compete with the microbiota. *Proc. Natl. Acad. Sci. U. S. A.* **108**, 17480–17485 (2011).
447 6. Spiga, L. *et al.* An Oxidative Central Metabolism Enables Salmonella to Utilize Microbiota-

448 Derived Succinate. *Cell Host & Microbe* **22**, 291-301.e6 (2017).

449 7. Winter, S. E. *et al.* Gut inflammation provides a respiratory electron acceptor for
450 Salmonella. *Nature* **467**, 426–429 (2010).

451 8. Cordes, T., Michelucci, A. & Hiller, K. Itaconic Acid: The Surprising Role of an Industrial
452 Compound as a Mammalian Antimicrobial Metabolite. *Annu. Rev. Nutr.* **35**, 451–473
453 (2015).

454 9. Yang, Z., Wang, H., Wang, Y., Ren, Y. & Wei, D. Manufacturing Multienzymatic Complex
455 Reactors In Vivo by Self-Assembly To Improve the Biosynthesis of Itaconic Acid in
456 Escherichia coli. *ACS Synth. Biol.* **7**, 1244–1250 (2018).

457 10. Zhao, M., Lu, X., Zong, H., Li, J. & Zhuge, B. Itaconic acid production in microorganisms.
458 *Biotechnol. Lett.* **40**, 455–464 (2018).

459 11. Hoyt, J. C., Robertson, E. F., Berlyn, K. A. & Reeves, H. C. Escherichia coli isocitrate lyase:
460 properties and comparisons. *Biochim. Biophys. Acta - Gen. Subj.* **966**, 30–35 (1988).

461 12. McFadden, B. A. & Purohit, S. Itaconate, an isocitrate lyase-directed inhibitor in
462 Pseudomonas indigofera. *J. Bacteriol.* **131**, 136–144 (1977).

463 13. Michelucci, A. *et al.* Immune-responsive gene 1 protein links metabolism to immunity by
464 catalyzing itaconic acid production. *Proc. Natl. Acad. Sci.* **110**, 7820–7825 (2013).

465 14. Strelko, C. L. *et al.* Itaconic Acid Is a Mammalian Metabolite Induced during Macrophage
466 Activation. *J. Am. Chem. Soc.* **133**, 16386–16389 (2011).

467 15. Naujoks, J. *et al.* IFNs Modify the Proteome of Legionella-Containing Vacuoles and
468 Restrict Infection Via IRG1-Derived Itaconic Acid. *PLoS Pathog.* **12**, e1005408 (2016).

469 16. Zhu, X. *et al.* Systemic responses of BALB/c mice to Salmonella typhimurium infection. *J.*

470 *Proteome Res.* **13**, 4436–4445 (2014).

471 17. Sasikaran, J., Ziemski, M., Zadora, P. K., Fleig, A. & Berg, I. A. Bacterial itaconate
472 degradation promotes pathogenicity. *Nat Chem Biol* **10**, 371–377 (2014).

473 18. Eriksson, S., Lucchini, S., Thompson, A., Rhen, M. & Hinton, J. C. Unravelling the biology
474 of macrophage infection by gene expression profiling of intracellular Salmonella enterica.
475 *Mol. Microbiol.* **47**, 103–118 (2003).

476 19. Srikumar, S. *et al.* RNA-seq Brings New Insights to the Intra-Macrophage Transcriptome
477 of Salmonella Typhimurium. *PLoS Pathog* **11**, e1005262 (2015).

478 20. Shi, L. *et al.* Proteomic analysis of Salmonella enterica serovar typhimurium isolated from
479 RAW 264.7 macrophages: identification of a novel protein that contributes to the
480 replication of serovar typhimurium inside macrophages. *J. Biol. Chem.* **281**, 29131–29140
481 (2006).

482 21. Santiviago, C. A. *et al.* Analysis of pools of targeted Salmonella deletion mutants
483 identifies novel genes affecting fitness during competitive infection in mice. *PLoS Pathog.*
484 **5**, e1000477 (2009).

485 22. Haneda, T., Ishii, Y., Danbara, H. & Okada, N. Genome-wide identification of novel
486 genomic islands that contribute to Salmonella virulence in mouse systemic infection.
487 *FEMS Microbiol. Lett.* **297**, 241–249 (2009).

488 23. Elder, J. R. *et al.* The Salmonella pathogenicity island 13 contributes to pathogenesis in
489 streptomycin pre-treated mice but not in day-old chickens. *Gut Pathog.* **8**, 16 (2016).

490 24. Espinoza, R. A. *et al.* Differential roles for pathogenicity islands SPI-13 and SPI-8 in the
491 interaction of Salmonella Enteritidis and Salmonella Typhi with murine and human

492 macrophages. *Biol. Res.* **50**, 5 (2017).

493 25. Pédelacq, J.-D., Cabantous, S., Tran, T., Terwilliger, T. C. & Waldo, G. S. Engineering and
494 characterization of a superfolder green fluorescent protein. *Nat. Biotechnol.* **24**, 79–88
495 (2006).

496 26. Alpuche Aranda C.M., Swanson, J. A., Loomis, W. P. & Miller, S. I. Salmonella
497 typhimurium activates virulence gene transcription within acidified macrophage
498 phagosomes. *Proc. Natl. Acad. Sci. U. S. A.* **89**, 10079–10083 (1992).

499 27. Rathman, M., Sjaastad, M. D. & Falkow, S. Acidification of phagosomes containing
500 Salmonella typhimurium in murine macrophages. *Infect. Immun.* **64**, 2765–2773 (1996).

501 28. Chakraborty, S., Mizusaki, H. & Kenney, L. J. A FRET-based DNA biosensor tracks OmpR-
502 dependent acidification of Salmonella during macrophage infection. *PLoS Biol.* **13**,
503 e1002116 (2015).

504 29. Mills, E. L. *et al.* Itaconate is an anti-inflammatory metabolite that activates Nrf2 via
505 alkylation of KEAP1. *Nature* **556**, 113–117 (2018).

506 30. Jha, A. K. *et al.* Network integration of parallel metabolic and transcriptional data reveals
507 metabolic modules that regulate macrophage polarization. *Immunity* **42**, 419–430
508 (2015).

509 31. Tallam, A. *et al.* Gene Regulatory Network Inference of Immunoresponsive Gene 1 (IRG1)
510 Identifies Interferon Regulatory Factor 1 (IRF1) as Its Transcriptional Regulator in
511 Mammalian Macrophages. *PLoS One* **11**, e0149050 (2016).

512 32. Jacobson, A. *et al.* A Gut Commensal-Produced Metabolite Mediates Colonization
513 Resistance to Salmonella Infection. *Cell Host & Microbe* **24**, 296-307.e7 (2018).

514 33. Ricke, S. C. Perspectives on the use of organic acids and short chain fatty acids as
515 antimicrobials. *Poult. Sci.* **82**, 632–639 (2003).
516 34. Tannahill, G. M. *et al.* Succinate is an inflammatory signal that induces IL-1β through HIF-
517 1α. *Nature* **496**, 238–242 (2013).
518 35. Hammerer, F., Chang, J. H., Duncan, D., Castaneda Ruiz, A. & Auclair, K. Small Molecule
519 Restores Itaconate Sensitivity in Salmonella enterica: A Potential New Approach to
520 Treating Bacterial Infections. *Chembiochem* **17**, 1513–1517 (2016).
521 36. Schmieger, H. A method for detection of phage mutants with altered transducing ability.
522 *Mol. Gen. Genet. MGG* **110**, 378–381 (1971).
523 37. Zou, S. B. *et al.* Loss of elongation factor P disrupts bacterial outer membrane integrity. *J.*
524 *Bacteriol.* **194**, (2012).
525 38. Datsenko, K. A. & Wanner, B. L. One-step inactivation of chromosomal genes in
526 Escherichia coli K-12 using PCR products. *Proc. Natl. Acad. Sci.* **97**, 6640–6645 (2000).
527 39. Cherepanov, P. P. & Wackernagel, W. Gene disruption in Escherichia coli: TcR and KmR
528 cassettes with the option of Flp-catalyzed excision of the antibiotic-resistance
529 determinant. *Gene* **158**, 9–14 (1995).
530 40. Gibson, D. G. *et al.* Enzymatic assembly of DNA molecules up to several hundred
531 kilobases. *Nat Meth* **6**, 343–345 (2009).
532 41. Corcoran, C. P. *et al.* Superfolder GFP reporters validate diverse new mRNA targets of the
533 classic porin regulator, MicF RNA. *Mol. Microbiol.* **84**, 428–445 (2012).
534 42. Urban, J. & Vogel, J. A green fluorescent protein (GFP)-based plasmid system to study
535 post-transcriptional control of gene expression in vivo. in *Riboswitches* (ed. Serganov, A.)

536 **540**, 301–319 (Humana Press, 2009).

537 43. Cooper, C. A. *et al.* Structural and biochemical characterization of SrcA, a multi-cargo
538 type III secretion chaperone in Salmonella required for pathogenic association with a
539 host. *PLoS Pathog* **6**, e1000751 (2010).

540 44. Coombes, B. K., Brown, N. F., Valdez, Y., Brumell, J. H. & Finlay, B. B. Expression and
541 secretion of Salmonella pathogenicity island-2 virulence genes in response to
542 acidification exhibit differential requirements of a functional type III secretion apparatus
543 and SsaL. *J. Biol. Chem.* **279**, 49804–49815 (2004).

544

Figures

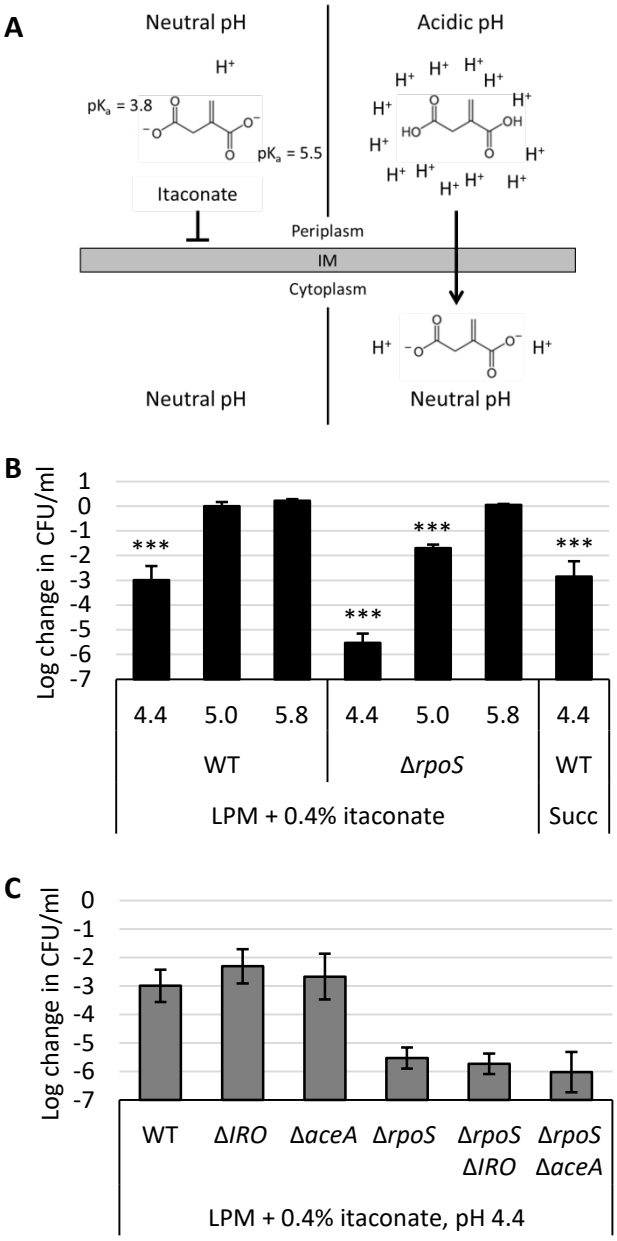

Figure 1: Itaconate is bactericidal at low pH. A) At neutral pH, the charges on itaconate inhibit diffusion across a lipid membrane (left). At acidic pH, itaconate protonates to itaconic acid, which can traverse the membrane (right). In the cytoplasm, itaconic acid dissociates and releases protons, trapping it in the cell and acidifying the cytoplasm. **B)** Survival (relative to 0h time point) of wild-type (WT) or *rpoS* mutant *Salmonella* after 3h in LPM media supplemented with 0.4% itaconate or succinate (Succ) and adjusted to pH 4.4, 5.0, or 5.8 as indicated. **C)** As in A but showing survival of *Salmonella aceA* and itaconate response operon (IRO) mutants in LPM + itaconate media at pH 4.4. All data are the average of at least three biological replicates and error bars show one standard deviation. A one-way ANOVA with Sidak's multiple comparison test was conducted comparing each sample to the same strain at pH 5.8 (B). WT in succinate was compared to WT at pH 5.8 in itaconate. Mutants in panel C were not significantly different than their parental strain (WT or Δ*rpoS*). ***, $p < 0.001$.

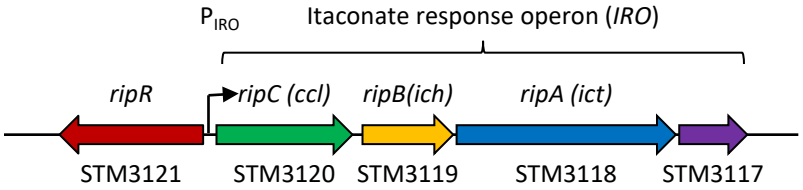

Figure 2: Overview of the itaconate degradation operon (IRO) and the itaconate-responsive regulator, *ripR.* *Salmonella* gene loci based on the genome of *Salmonella* Typhimurium LT2 are shown below. Identities of *ccl*, *ich*, and *ict* are shown above as previously reported (17). STM3117 appears to be encoded in the same operon however its function remains unknown. In this work we designate the names '*ripR*' for STM3121, 'itaconate response operon' (IRO) for STM3120-STM3117, and 'P_{IRO}' for the IRO promoter.

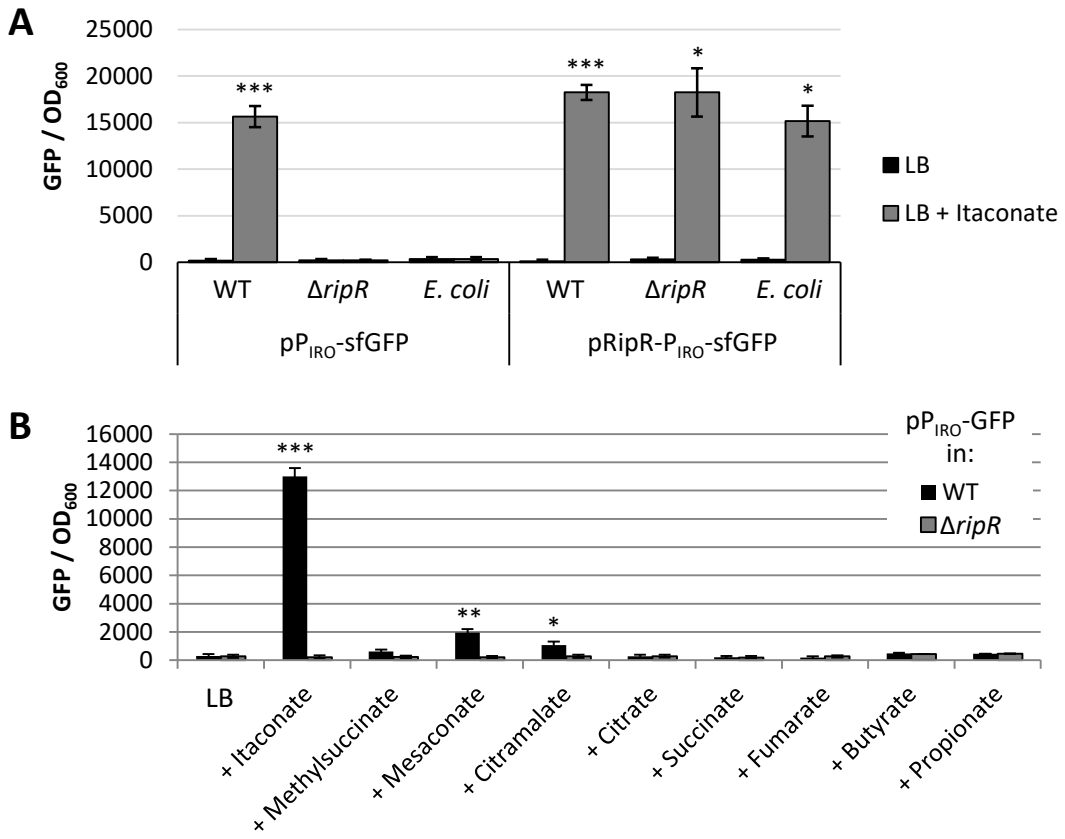

Figure 3: RipR is necessary and sufficient to induce P_{IRO} expression in response to itaconate. Expression of P_{IRO}-sfGFP in wild-type (WT) or *ripR* knockout (Δ*ripR*) *Salmonella*, or in *E. coli*. Figures show GFP fluorescence normalized to optical density at 600nm (OD_{600}) after 16h of growth in LB alone or supplemented with 0.2% itaconate (A) or similar metabolites (B). Data are the average of at least three biological replicates and error bars show one standard deviation. pP_{IRO}, plasmid-borne transcriptional fusion of P_{IRO} to sfGFP; pRipR-P_{IRO}, pP_{IRO} with the *ripR* gene and its native promoter included on the plasmid. A Games-Howell ANOVA was conducted comparing with and without itaconate for each strain (A), or comparing WT to Δ*ripR* (B) for each added metabolite. *, $p < 0.05$; **, $p < 0.01$; ***, $p < 0.001$.

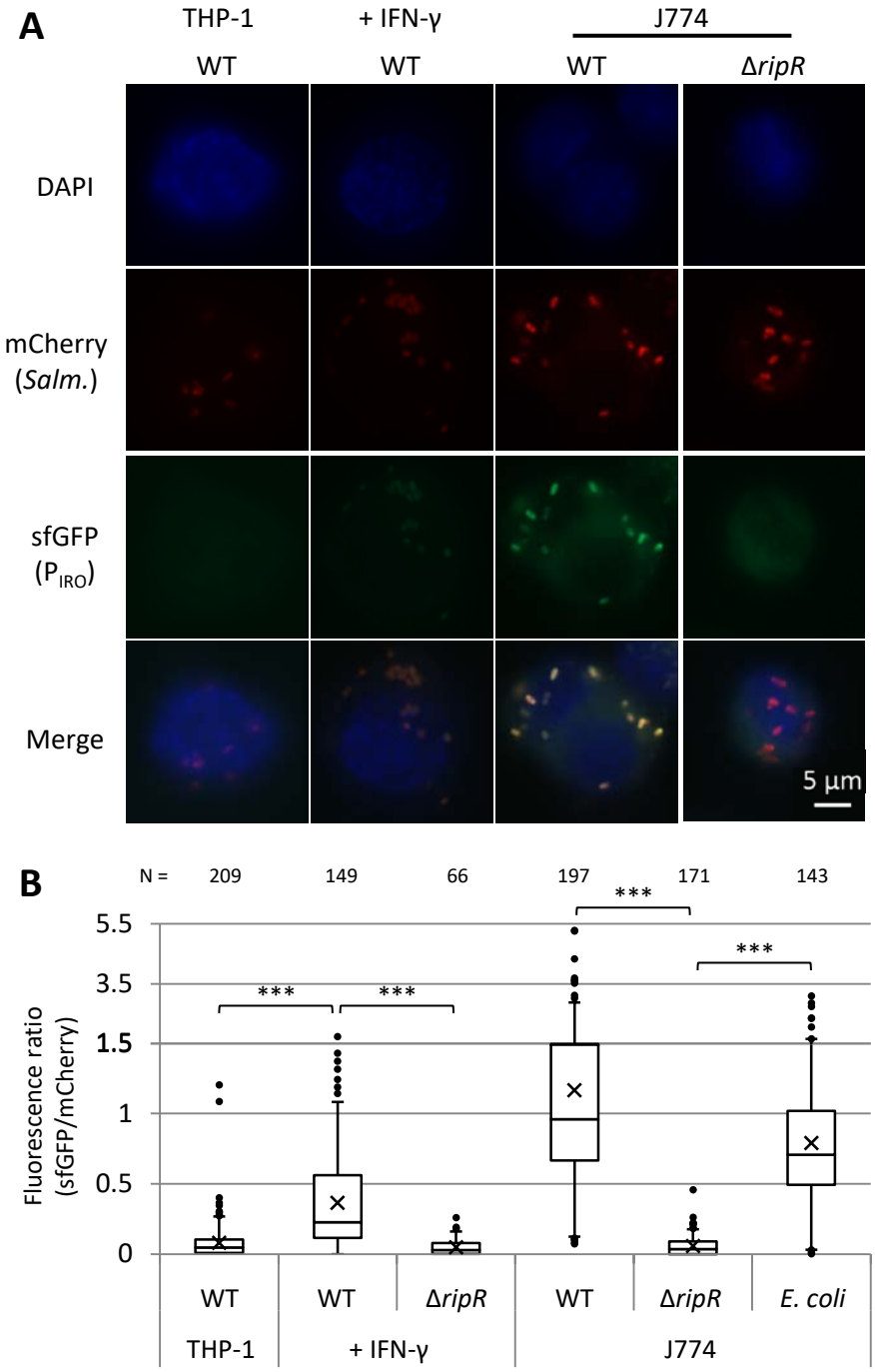

Figure 4: P_{IRO} is activated in J774 macrophage and THP-1 macrophage stimulated with IFN-γ. Expression of P_{IRO}-sfGFP in intracellular wild-type (WT) or *ripR* knockout (Δ*ripR*) *Salmonella* containing the pICM-P_{IRO} plasmid (constitutive mCherry expression). For expression in *E. coli,* the *ripR* gene was also encoded on the reporter plasmid. '+ IFN-γ' samples were pre-treated with human IFN-γ. **A)** Representative fluorescence microscopy images. **B)** Relative fluorescence quantification of individual bacterial particles at 8h post-infection. Number of bacteria quantified is indicated above and totalled from at least two biological replicates (≥ 3 for all WT *Salmonella* samples). Boxes indicate first and third quartiles; central line, median; X, mean; whiskers, 95th percentile; dots, all non-zero data points outside 95th percentile. The y-axis changes scale at 1.5 to better show outliers. A Games-Howell ANOVA was conducted comparing indicated samples. ***, $p < 0.001$.

Supplemental Figures

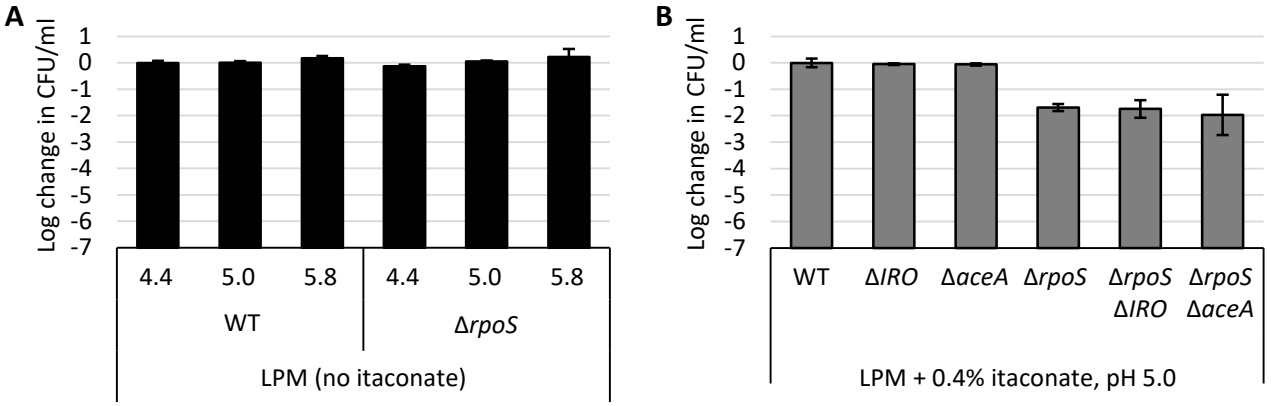

Figure S1: pH 4.4 without itaconate was not bactericidal. A) Survival (relative to 0h time point) of wild-type (WT) or *rpoS* mutant *Salmonella* after 3h in LPM media adjusted to pH 4.4, 5.0, or 5.8 as indicated. **B)** Survival of *Salmonella aceA* and itaconate response operon (IRO) mutants in LPM + itaconate media at pH 5.0. All data are the average of at least three biological replicates and error bars show one standard deviation.

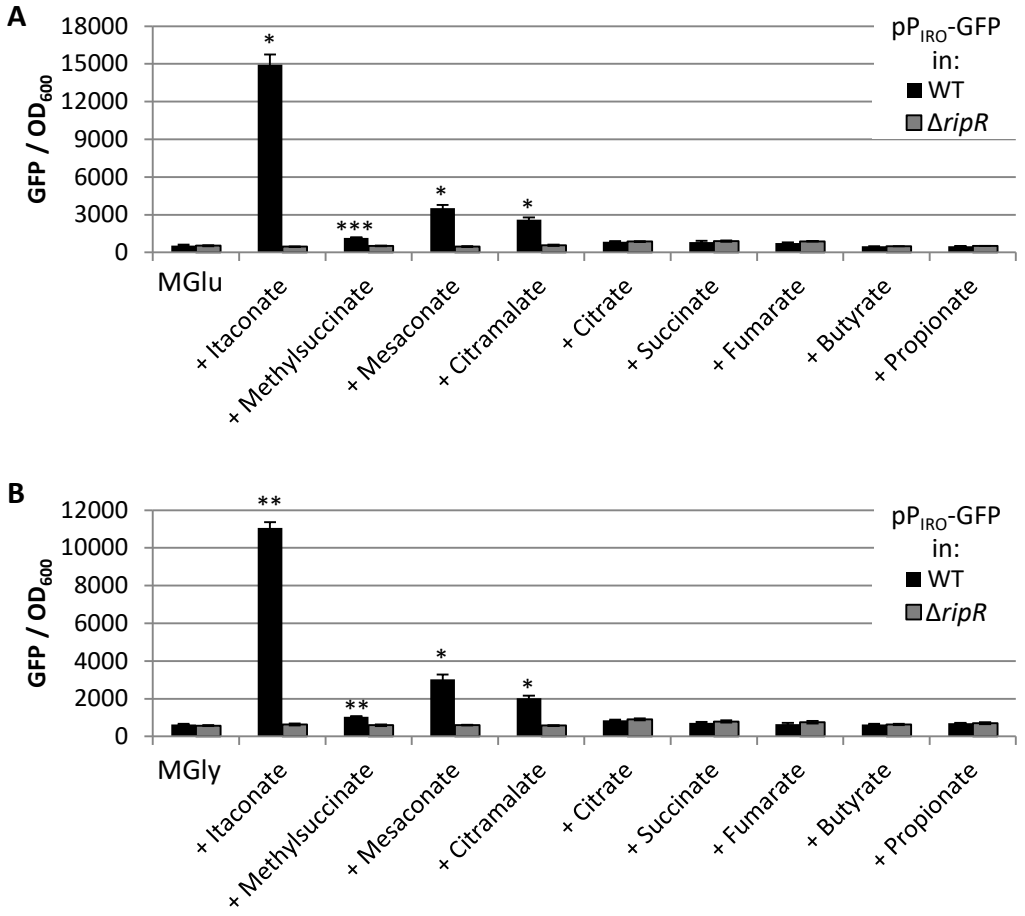

Figure S2: Itaconate induction of P_{IRO} occurs in minimal media. Expression of P_{IRO}-sfGFP in wild-type (WT) or *ripR* knockout (Δ*ripR*) *Salmonella* as in Figure 1 except grown in MOPS minimal media with 0.2% Glucose (**A**; MGlu) or Glycerol (**B**; MGly) instead of LB. Data show GFP fluorescence normalized to OD_{600} after 16h of growth and are the average of at least three biological replicates. Error bars show one standard deviation. pP_{IRO}, plasmid-borne transcriptional fusion of P_{IRO} to sfGFP. A Games-Howell ANOVA was conducted comparing WT to Δ*ripR* for each added metabolite. *, $p < 0.05$; **, $p < 0.01$; ***, $p < 0.001$.

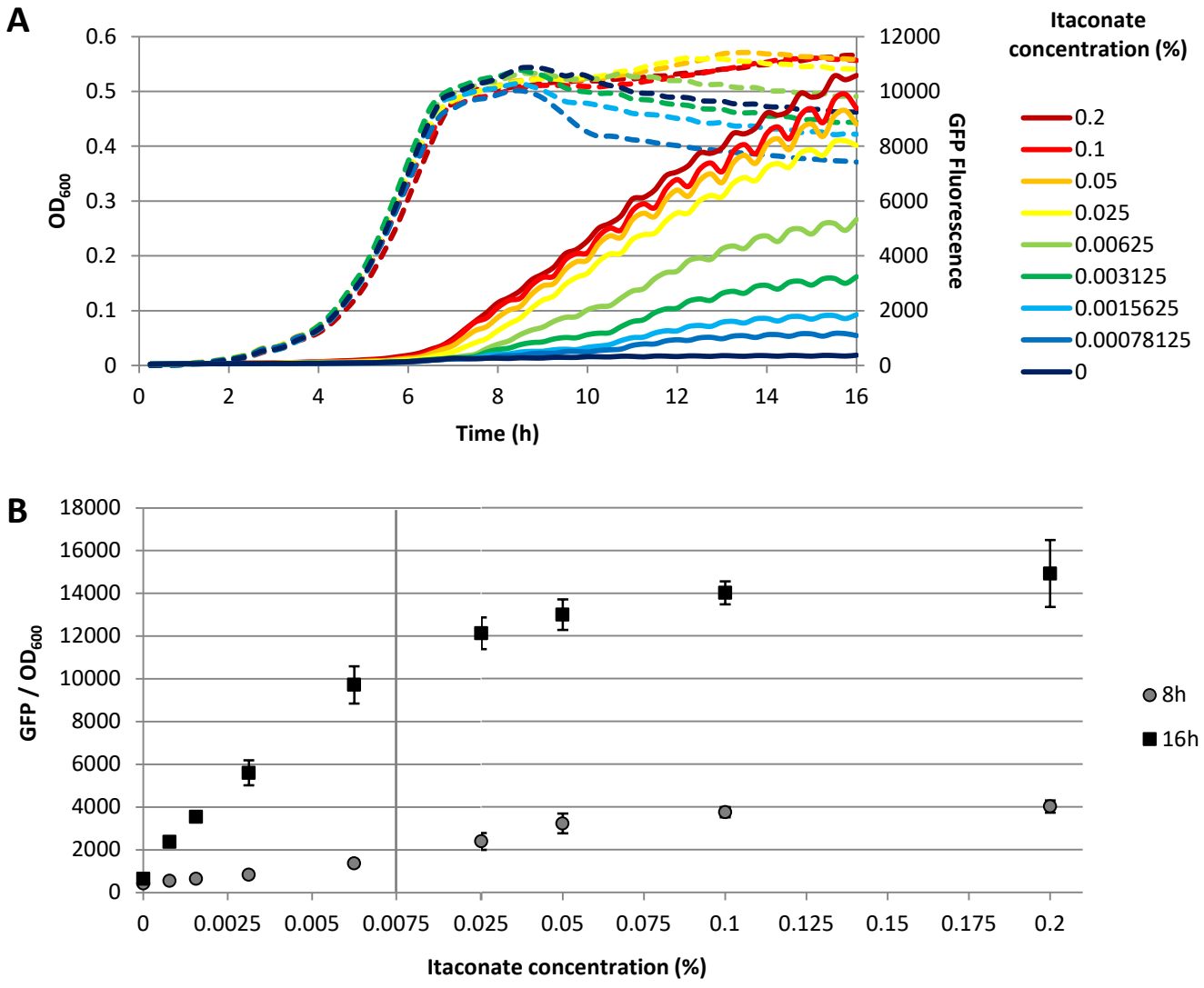

Figure S3: P_{IRO} is induced by itaconate in a dose-dependent manner. A) Example replicate showing *Salmonella* optical density (dashed lines) and P_{IRO}-sfGFP fluorescence (solid lines) for a range of itaconate concentrations across 16h of growth. All conditions were in MOPS minimal media with 0.2% glucose as a carbon source and indicated concentration of itaconate (%, g/100ml). **B)** Average P_{IRO}-sfGFP fluorescence (normalized to OD_{600}) at 8h or 16h across two biological replicates. Error bars indicate one standard deviation. The x-axis changes scale at 0.0075% to show lower concentrations more clearly.

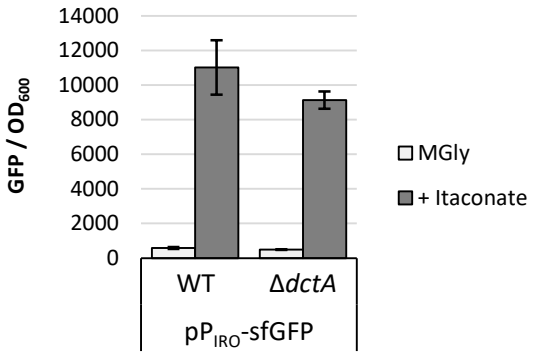

Figure S4: DctA is not required for the response to itaconate. Expression of P_{IRO}-sfGFP in wild-type (WT) or *dctA* knockout (Δ*dctA*) *Salmonella*. Figure shows GFP fluorescence normalized to optical density at 600nm (OD_{600}) after 16h of growth in MOPS minimal media with 0.2% glycerol as the carbon source. Data are the average of at least two biological replicates and error bars show one standard deviation. pP_{IRO}-sfGFP*,* plasmid-borne transcriptional fusion of P_{IRO} to sfGFP.

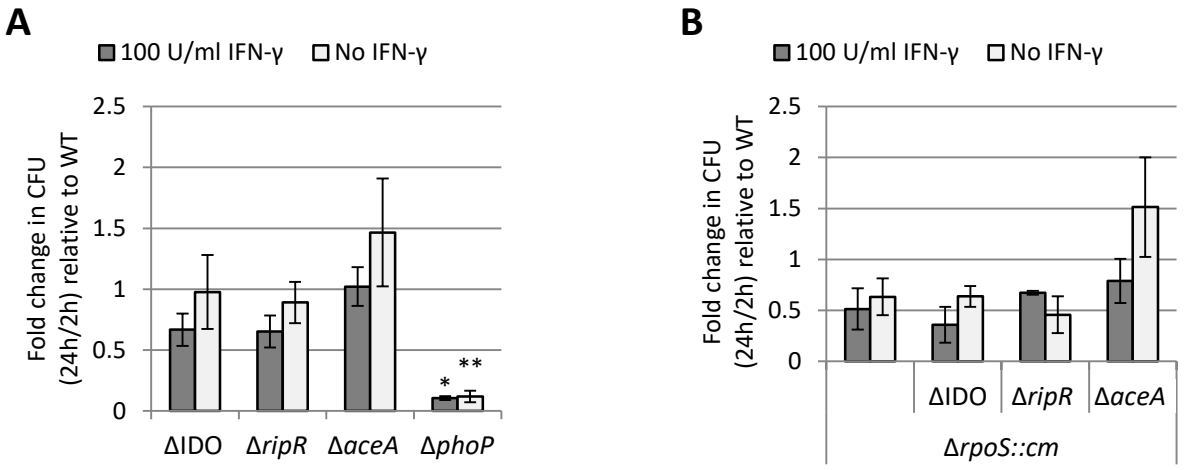

Figure S5: Survival of *Salmonella* mutants in J774 macrophage with and without IFN-γ stimulation relative to wild-type. The fold change in CFU recovered (24h relative to 2h post-infection) is shown and data from each replicate was normalized to the 24h/2h ratio obtained for wild-type *Salmonella*. Columns show the average of three biological replicates and error bars show one standard error of the mean. Since samples were normalized to wild-type in each replicate, a one-way ANOVA with Sidak's multiple comparison test was conducted comparing each strain to the Δ*aceA* strain (A) or to the Δ*rpoS* strain (B). Only the Δ*phoP* mutant was found to have a $p < 0.05$. *, $p<0.05$; **, $p < 0.01$.

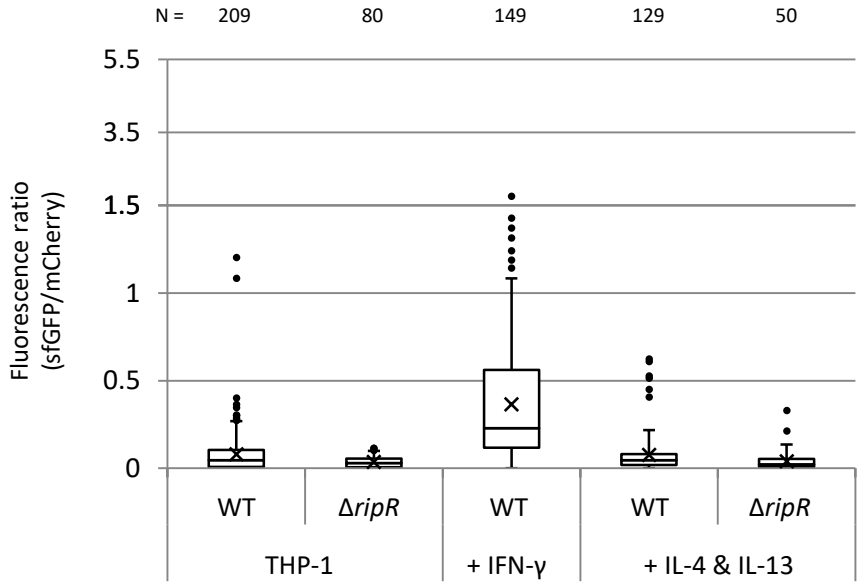

Figure S6: P_{IRO} shows little-to-no activation in THP-1 macrophage stimulated with IL-4 and IL-13. As in Figure 4, expression of P_{IRO}-sfGFP in intracellular wild-type (WT) or *ripR* knockout (Δ*ripR*) *Salmonella* containing the pICM-P_{IRO} plasmid (constitutive mCherry expression). THP-1 macrophage were pre-treated with no stimulant, human IFN-γ, or IL-4 and IL-13 and infected with *Salmonella* for 8h. Data for WT *Salmonella* in THP-1 with no treatment or IFN-γ are shown in Figure 4 and are shown again here for comparison. As in Figure 4, data shows relative fluorescence quantification of individual bacterial particles. Number of bacteria quantified is indicated above and totalled from at least three biological replicates. Boxes indicate first and third quartiles; central line, median; X, mean; whiskers, 95th percentile; dots, all non-zero data points outside 95th percentile. The y-axis changes scale at 1.5 to better show outliers.